

Diffusion in the Anderson model of a disordered system: A numerical study

P. Prelovšek

*Physik Department der Technischen Universität München, 8046 Garching, West Germany
and Department of Physics, J. Stefan Institute, University of Ljubljana, 61001 Ljubljana, Yugoslavia*

(Received 27 April 1978)

Anderson's model for a disordered system is studied numerically by a direct simulation of the particle diffusion on the two-dimensional square lattice. The energy-dependent diffusivity and the participation ratio are evaluated in extended regime for various sets of band energies and disorder parameters. Far from the mobility edges our results are qualitatively consistent with the coherent-potential approximation, which is shown to generally overestimate the diffusivity. In the critical regime, our data indicate a continuous nearly linear variation of the diffusivity and thus contradict the concept of minimum metallic conductivity. The participation ratio also reveals a critical dependence. The results are interpreted in terms of classical percolation character of the particle diffusion near the mobility edges.

I. INTRODUCTION

Mott's notion¹ of the existence of mobility edges, which in a disordered system separate the energy regions of extended and localized states, has been supported by a number of theoretical and numerical investigations in the past decade.² It has also been recognized that the behavior in the vicinity of mobility edges has a relationship to the phase-transition problems. Various renormalization-group approaches which employed this analogy have been presented recently.³⁻⁵ Further progress in this direction would be facilitated if one would have a list of critical quantities and at least a qualitative understanding of their critical behavior. The localized side of the transition is at present better understood since it proved to be more amenable to the theoretical² and numerical studies.⁶⁻⁹ The situation in the extended regime is much more controversial. For the conductivity, which is the central quantity in this region, a discontinuous behavior was originally proposed.^{1,7} Cohen and Jortner¹⁰ argue for a continuous variation analogous to classical percolation. More recent arguments by Mott¹¹ also seem to contradict the concept of minimum metallic conductivity. At the same time, Licciardello and Thouless¹² claim that in a disordered system the conductivity should be always zero, in a strict sense. Numerical studies of the conductivity, as well as of other presumable critical quantities in the extended regime, like the participation ratio,⁹ were until now only of a qualitative character,^{6,13} or yielded indirect information.^{7,12} Results would be desirable also outside the critical regime, where the validity of theoretical treatments like the coherent-potential approximation (CPA)¹⁴ should be tested.

In this paper, we present the results of our nu-

merical investigations of the extended regime in the Anderson model for a disordered solid. The study was performed for the two-dimensional (2D) square lattice and the emphasis was put on the critical regime. The basic idea of our approach is to simulate directly the quantum-mechanical diffusion of a particle with a well-defined energy and to extract from the simulation data quantities of interest, i.e., the conductivity, the participation ratio, the coherence length, etc. Some conclusions have already been reported in our recent letter.¹⁵

The organization of the paper is as follows: In Sec. II we discuss the relationship between the energy-dependent conductivity and the diffusivity in the extended regime. In Sec. III technical details of our simulation approach as well as our method of data analysis are described. Section IV is devoted to the presentation and discussion of results for the diffusivity and the participation ratio. In Sec. V, an interpretation of our critical-regime data via classical percolation is given.

II. CONDUCTIVITY AND DIFFUSIVITY

We study the disordered system with the Hamiltonian, as it was originally introduced by Anderson,¹⁴

$$H = \sum_i \epsilon_i c_i^\dagger c_i + \sum_{i,j} V_{ij} c_i^\dagger c_j, \quad (1)$$

where $c_i^\dagger(c_i)$ are the creation (annihilation) operators for a particle on the lattice site i . The site energies ϵ_i are uniformly distributed within the interval $-\frac{1}{2}W < \epsilon_i < \frac{1}{2}W$, while the transfer integrals $V_{ij} = V$ connect nearest neighbors.

To calculate the energy-dependent conductivity $\sigma(E)$, defined by the relation

$$\sigma = - \int \frac{df(E)}{dE} \sigma(E) dE, \quad (2)$$

where $f(E)$ is the Fermi-Dirac distribution function, we employ its connection to the energy-dependent diffusivity $D(E)$ for the case of the noninteracting Fermi gas,

$$\sigma(E) = 2e^2 n(E) D(E) / \Omega. \quad (3)$$

$n(E)$ denotes the normalized density of particle states, Ω is the cell volume, whereas the factor 2 which takes into account the spin degeneracy has been introduced for consistency with other authors. Equation (3) can be deduced from the formalism of Kudinov and Firsov.¹⁶ They proved, for the case of a small concentration of mobile electrons,

$$\sigma = \frac{2e^2\beta}{N_0\Omega} \lim_{t \rightarrow \infty} \frac{1}{2t} \sum_{i,j} (r_i^\alpha - r_j^\alpha)^2 \times \langle \langle c_i^\dagger(t) c_i(t) c_j^\dagger c_j \rangle \rangle_c. \quad (4)$$

Here, $\beta = 1/k_B T$, \vec{r}_i is the site vector, and N_0 the number of lattice sites. $\langle \langle \rangle \rangle_c$ denotes the thermodynamic and configurational average. Equation (4) relates σ and the diffusion constant. Eliminating the thermodynamic average in (4) in the same way as in (2), we arrive at expression (3) [note $\beta f(E) \sim -df(E)/dE$], which for disordered systems was also pointed out by Butcher.¹⁷

Theoretical investigations of $\sigma(E)$ and $D(E)$ in the extended regime start usually from the representation

$$D(E) = -\frac{1}{n(E)\pi} \sum_{j,k,i} (r_i^\alpha - r_j^\alpha)(r_k^\alpha - r_i^\alpha) V_{ij} V_{ki} \times \langle \langle \text{Im} G_{ii}(E) \text{Im} G_{jk}(E+0) \rangle \rangle_c, \quad (5)$$

where $G_{ii}(z) = \langle c_i(z-H)^{-1} c_i^\dagger \rangle$. Within CPA¹⁴ the configurational average in (5) can be decoupled into a product of averaged one-particle Green's functions, whereby $\langle G_{ii}(E) \rangle_c$ and $n(E)$ are calculated self-consistently. CPA thus neglects all statistical phase as well as amplitude correlations between the E and $E+0$ particle states in Eq. (5). The Mott-Hindley¹⁸ value for the minimum metallic conductivity is based on a similar assumption, where also the coherence length is set to zero, i.e.,

$$\langle \text{Im} G_{ij}(E) \rangle_c = \pi n(E) \delta_{ij}, \quad (6)$$

$$D_{\text{MH}}(E) = 2\pi a_0^2 V^2 n(E).$$

Equation (6) is given for the case of a 2D square lattice where a_0 denotes the lattice parameter. However, it has been shown by the author¹⁹ that in the vicinity of mobility edges the correlation corrections to CPA could decrease $D(E)$ considerably and seem to allow lower values than (6).

III. NUMERICAL SIMULATION METHOD

Our simulation procedure is derived into two steps: (a) To obtain a wave packet with a well-defined energy E , we first find in a smaller subsystem for the generated configuration of ϵ_i an exact eigenfunction of the Hamiltonian (1), i.e., $\psi_m(\vec{r}_i)$ with $E_m \sim E$. To reduce the storage and time requirements we use the diagonalization for band matrices, which yields for given E only the closest eigenvalue with the corresponding eigenvector.²⁰ The modulated $\psi_m(\vec{r}_i)$,

$$\varphi(\vec{r}_i, t=0) = c \exp(-|\vec{r}_i - \vec{r}_0|^2 / 4\rho^2) \psi_m(\vec{r}_i), \quad (7)$$

represents the initial condition for diffusion in the enlarged system. Now, $\varphi(\vec{r}_i, t=0)$ corresponds only to an approximate eigenstate. Its energy resolution σ_E can be evaluated directly,

$$\sigma_E^2 = \langle \varphi | H^2 | \varphi \rangle - \langle \varphi | H | \varphi \rangle^2. \quad (8)$$

In Eq. (7), we choose the parameter ρ so that σ_E is minimized. σ_E is in the extended regime predominantly determined by the dimensions of the subsystem. In our calculations, which involve $21 \times 21 = 441$ sites, we obtain $\sigma_E \sim 0.3V$. In the vicinity of mobility edges, the functions $\psi_m(\vec{r}_i)$ exhibit large amplitude fluctuations and become more insensitive to boundary conditions.⁷ This manifests itself in larger variations among σ_E values. By selection we are thus able to achieve in this regime $\sigma_E < 0.2V$. (b) The evolution of $\varphi(\vec{r}_i, t)$ is then followed by the numerical integration of the time-dependent Schrödinger equation, for which we employ the fourth-order Runge-Kutta procedure. The dimensions of the 2D system are increased steadily, under the condition that the boundaries do not significantly influence the results. At most, our sample contains $100 \times 100 = 10^4$ sites. The time step is predominantly dictated by the stability of σ_E and proved to be strongly dependent on E . We thus reach, in the low-diffusivity regime, $t \sim 300/V$ at $E=0$ (band center) and $t \sim 150/V$ at band edges $E/V \sim 4$. Note that we are using the convention $\hbar=1$ throughout the paper. Finally, the diffusivity is evaluated using the relation (4)

$$D(E) = \lim_{t \rightarrow \infty} \langle R^2(t) \rangle / 4t \quad (9)$$

with

$$\langle R^2(t) \rangle = \sum_i r_i^2 [|\varphi(\vec{r}_i, t)|^2 - |\varphi(\vec{r}_i, 0)|^2]. \quad (10)$$

The extrapolation in Eq. (9) is performed graphically, since we observe from the $\langle R^2(t) \rangle$ curves that after a transient time, which is predominantly a function of disorder, a steady-diffusion state with a well-defined linear variation of $\langle R^2(t) \rangle$ is

reached.

Further information about the nature of extended states can be extracted from our simulation data via functions

$$Z_n(\vec{r}, t) = \sum_i [\varphi(\vec{r}_i, t) \varphi^*(\vec{r}_i + \vec{r}, t)]^n. \quad (11)$$

We are able to calculate from $Z_1(\vec{r}, t)$ the coherence length, the $Z_n(\vec{r}=0, t)$ are related to the wavefunction amplitude fluctuations, etc. Usually, analogous quantities $F_n(\vec{r})$ are defined directly for the exact eigenstates $\psi_m(\vec{r}_i)$ of the system. The participation ratio,⁹ which in the extended regime represents the effective fraction of sites occupied by the eigenfunction $\psi_m(\vec{r}_i)$, can be thus expressed as $P = [N_0 F_2(\vec{r}=0)]^{-1}$. Although the $Z_n(\vec{r}, t)$ in Eq. (11) are not identical to $F_n(\vec{r})$, we can establish their relation by extending the diffusion ansatz (7) to arbitrary t with $\rho^2 = \langle R^2(t) \rangle$. Now, $\psi_m(\vec{r}_i) = \psi'(\vec{r}_i, t)$ in Eq. (7) corresponds only to an approximate extended eigenfunction of the whole system. It seems also plausible that the Gaussian function is statistically uncorrelated to $\psi'(\vec{r}_i, t)$. The validity of the ansatz can be partly tested by identities stemming from (7), e.g., $K_1 = \langle R^4(t) \rangle / 2 \langle R^2(t) \rangle^2 = 1$, etc. In our calculations, we observe larger deviations due to unsteady diffusion only in the low-diffusivity regime, where $0.9 < K_1 < 1.4$. With the help of expression (7) we can evaluate all $F_n(\vec{r})$. For example,

$$\begin{aligned} P &= \lim_{t \rightarrow \infty} a_0^2 [2\pi \langle R^2(t) \rangle Z_2(\vec{r}=0, t)]^{-1} \\ &= a_0^2 D_N(E) / 8\pi D(E), \end{aligned} \quad (12)$$

where

$$D_N(E) = \lim_{t \rightarrow \infty} [t Z_2(\vec{r}=0, t)]^{-1}. \quad (13)$$

Our resolution in W can be estimated from the effective number of sites $N_{\text{eff}} \sim 2\pi \langle R^2(t) \rangle$. Since in most cases we are limited to $\langle R^2(t_{\text{max}}) \rangle = 500 a_0^2$, it follows that $\sigma_w/W \sim 1/(N_{\text{eff}})^{1/2} \sim 0.02$. Our method could be used as well for the study of the localized regime, where $D(E) = 0, D_N(E) = 0$, etc. There, $\langle R^2(t) \rangle$ and $Z_n(\vec{r}, t)$ approach or oscillate around some stationary value specified by the given configuration. To gain, besides the qualitative, also some quantitative information about physical quantities like the localization length and the participation ratio, it would be essential to perform an averaging over a number of different configurations, which would make this approach rather inefficient.

IV. RESULTS AND DISCUSSION

Our diffusion simulations were performed for the following cases: (a) at fixed $E=0$ (center of the band) and $E/V=3$ the degree of disorder was

varied, $W/V=2.5-7$; (b) at fixed $W/V=5$ and $W/V=6$ for $E/V=0-4$. Note that the situation in the square lattice is symmetrical around $E=0$. The example selection was guided by the approximately known locations of the mobility edges $E_c(W)$,⁷ where the best available values stem from the work of Yoshino and Okazaki,⁸ i.e., $W_c(E=0) \sim 6.5V$ and $E_c(W=6V) \sim 3.2V$. The case (a) with $E/V=3$ was chosen to represent the points where in the weak-scattering regime the maximum conductivity occurs. The numerical procedure strongly favors example (a) with $E=0$ since, owing to a symmetrical situation, the numerical stability is substantially increased (a time step at least five times larger than in other examples is sufficient). Furthermore, the requirements on σ_E are rather modest due to the smooth variation of all quantities with E .

In Figs. 1(a) and 1(b) we present for the $E=0$ case some characteristic $\langle R^2(t) \rangle$ as well as the corresponding $N(t) = [Z_2(\vec{r}=0, t)]^{-1}$ curves. All presented W/V correspond to the extended region. In the weak-scattering examples, $W/V < 3$, the wave packet exhibits an accelerated expansion at short times and rather large volumes are needed to reach the diffusion regime, which effectively prevents an accurate study of $W/V < 2.5$. For larger $W/V > 4$ the steady-diffusion state is observed after a transient time τ , which seems to be determined mainly by the corresponding effective number of contributing sites $N(t) \sim 150-300$. Since $D_N(E)$ reduces strongly in the vicinity of mobility edges and, moreover, we claim the vanishing of P at $W_c(E)$, the condition $t \gg \tau$ is increasingly difficult to meet for the most critical examples (e.g., at $E=0$ for $W/V > 6.2$). Nevertheless, as seen in Fig. 1(a), the fluctuations around the ideal linear behavior are rather modest except at $W/V \sim 6.5$. We also do not observe any clear indications of saturation in the $\langle R^2(t) \rangle$ curves, which would confirm the recent conjecture of Licciardello and Thouless¹² that the eigenstates are always localized in two dimensions, independent of W/V . Note that $\langle R^2(t_{\text{max}}) \rangle$ are already large enough that these effects should become visible for $W/V > 5.5$, at least for localization-length values as presented in Ref. 12. Thus, at $W/V=6$ the presumable localization volume should be approximately equal to our effective volume $N_{\text{eff}} a_0^2$.

On the contrary, $N(t)$ curves reveal considerable deviations from the ideal behavior already for relatively weak disorder. Large fluctuations and at the same time small values of $D_N(E)$ prevent an accurate analysis for $W/V > 5$ and do not allow any reliable location of W_c via the condition $D_N(E) = 0$. This phenomenon by itself seems to favor a smeared-out transition or an inhomogen-

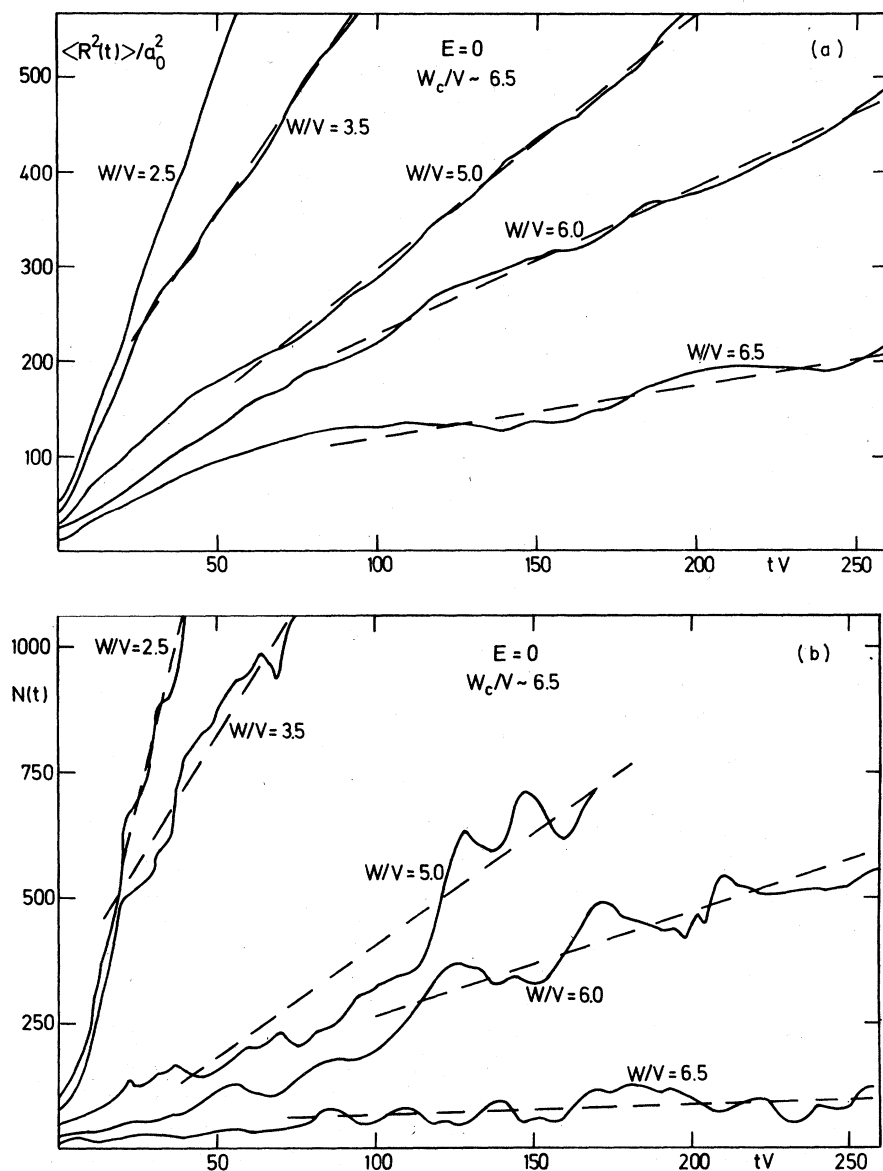


FIG. 1. Characteristic examples for the time dependence of (a) $\langle R^2(t) \rangle$ and (b) the corresponding $N(t) = [Z_2(\vec{r}=0, t)]^{-1}$ are plotted for various W/V in the extended regime at fixed $E=0$. Dashed lines represent graphical derivatives as used for the evaluation of $D(E)$ and $D_N(E)$ via Eqs. (9) and (13), respectively.

eous energy regime,¹¹ where the localized and extended states would coexist. Such interpretation is however inconsistent with rather well-defined values of $D(E)$.

In Figs. 2(a) and 2(b) our results for $D(E)$ at $E=0$ and $E/V=3$ are plotted. The circles denote the values obtained from independent configurations. We present also the corresponding CPA result¹⁴ as calculated from (5) as well as the Mott-Hindley values for the minimum metallic diffusivity from Eq. (6). In the evaluation of (6), we used the CPA results for $n(E)$ which are for our examples close to the exact ones.⁷

The scatter of data remains rather modest also

in the low-diffusivity region except for $W/V > 6$, where we could not guarantee $t \gg \tau$. For the weak-scattering regime $W/V < 4$ our results confirm the reliability of CPA. Consistent with the theory¹⁹ they also indicate that CPA generally overestimates the diffusivity. For $W/V > 4.5$ CPA fails qualitatively. Thus, the $D_{MH}(E)$ curves are crossed at $W/V = 4.5$ and $W/V = 5.5$, respectively. It must be mentioned that we are able to test separately the validity of the decoupling approximation to Eq. (5) as well as the value of coherence length. From the calculated $\lim_{t \rightarrow \infty} Z_1(\vec{r}_{ij}, t) = \langle m G_{ij}(E) \rangle_c / \pi n(E)$ we can evaluate the coherence corrections¹⁹ to $D_{MH}(E)$ in Eq. (6) by summing the largest con-

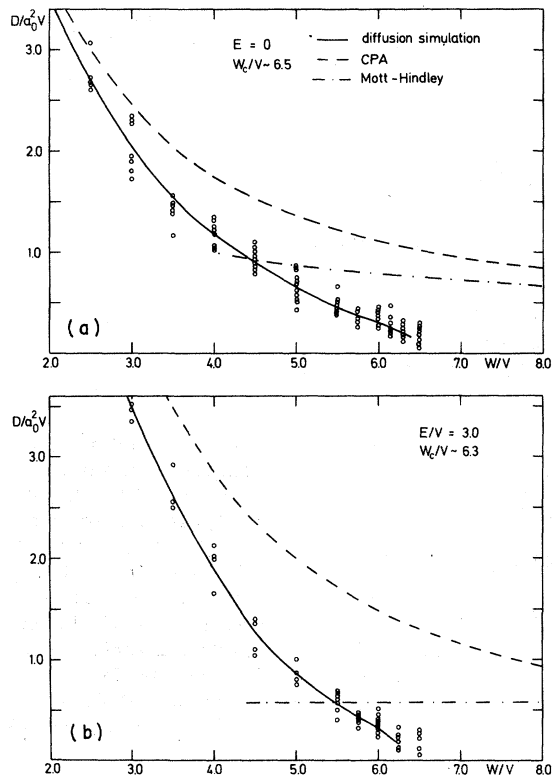


FIG. 2. Diffusivity $D(E)$ as a function of disorder parameter W/V at (a) $E=0$ and (b) $E/V=3$. Circles denote the results as obtained from different configurations. Plotted are also the corresponding CPA curve as well as the Mott-Hindley values for the minimum metallic diffusivity.

tributions to the sum in Eq. (5) where the decoupling is assumed for the Green's-function product. In the case $W/V=6$, e.g., the corrections still amount to 10% and 60% on the corresponding $D_{MH}(E)$ values for $E=0$ and $E/V=3$, respectively.

At $W/V \sim 5.5$ for both cases the value corresponding via Eq. (3) to $\sigma(E)=0.12e^2$ is reached. This figure was claimed by Licciardello and Thouless⁷ as the minimum metallic conductivity in two dimensions. In their recent work,¹² they correct their previous arguments and present new results which are consistent with ours at least for $W/V=6$, i.e., $\sigma(E=0)=0.078e^2$ (our value: $0.094e^2$), and $\sigma(E=3V)=0.058e^2$ ($0.063e^2$). Nevertheless, it seems that some systematic errors are still possible within their approach, since for the other set $W/V=4.5$ the discrepancy between the values is beyond the numerical errors of both methods, e.g., $\sigma(E=0)=0.158e^2$ (our result: $0.26e^2$) and $\sigma(E=3V)=0.132e^2$ ($0.224e^2$). From Figs. 2(a) and 2(b) we can set the upper bound to the presumable minimum metallic conductivity in two dimensions

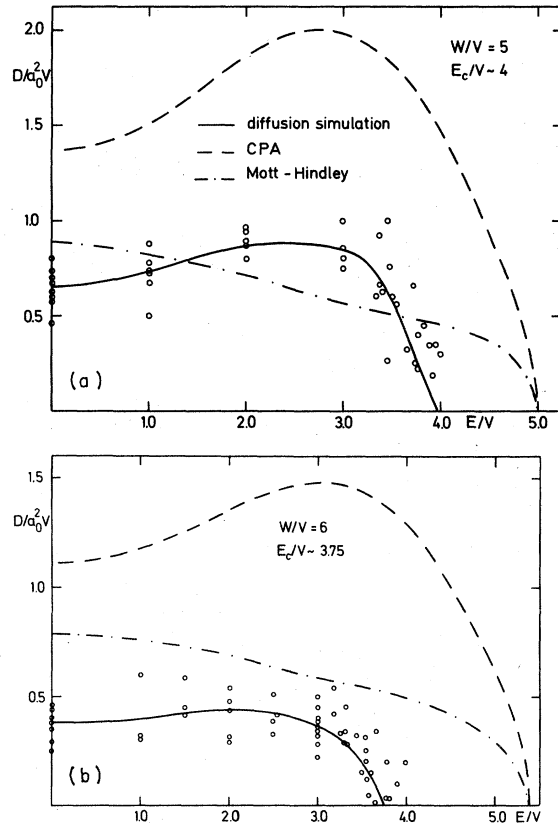


FIG. 3. $D(E)$ as a function of E/V at (a) $W/V=5$ and (b) $W/V=6$. The designation of the curves is the same as in Fig. 2. The values of E_c/V are estimated from our data.

$\sigma_m < 0.04e^2$. Since such a small step could be hardly defended theoretically, at least in the sense of the original Mott's arguments,¹ we would interpret our results by a continuous variation $D(E) \propto (W_c - W)^s$ in the critical regime $|W_c - W| < V$. For the Yoshino and Okazaki⁸ value $W_c(E=0)=6.5V$ we would obtain $s \sim 0.7$. It seems, however, likely that their analysis slightly underestimates W_c . Therefore, we cannot exclude the possibility $s \geq 1$, which could correspond to the classical-percolation critical exponent in two dimensions.²¹

In Figs. 3(a) and 3(b) we plot the $D(E)$ results at fixed $W/V=5$ and $W/V=6$. Both cases correspond to the strong-scattering regime. CPA curves grossly overestimate $D(E)$ and also reveal maxima at $E/V \sim 3$ which are in our results only weakly pronounced. Again, we observe that for $W/V=6$ $D(E) < D_{MH}(E)$ for all E . From Figs. 3(a) and 3(b) conclusions about the critical variation are more ambiguous. The rather steep E dependence is to some extent smeared out by our resolution $\sigma_E \sim 0.2V$. Nevertheless, we cannot recognize any

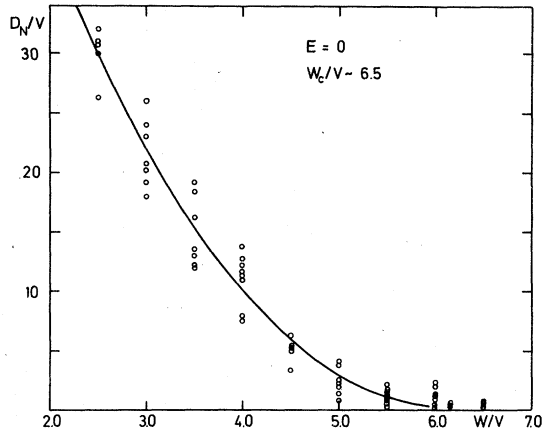


FIG. 4. D_N/V as a function of W/V at $E=0$. Circles denote the results obtained from different configurations.

contradiction with the continuous-variation assumption. We must also mention the difference between our $E_c/V \sim 3.75$ at $W/V=6$ and the value $E_c/V \sim 3.2$ Yoshino and Okazaki⁸ which seems questionable on account of the extensive extrapolation used in their procedure.

It has been realized from Fig. 1(b) that an analysis of $D_N(E)$ is less accurate. The results at $E=0$ plotted in Fig. 4 reveal a large scatter of data especially for $W/V > 5$, where the evaluation of $D_N(E)$ becomes more subjective. In spite of this, the qualitative difference between the $D(E)$ and $D_N(E)$ behavior becomes evident in the critical regime $W/V > 4.5$. A physical interpretation can be given via the participation ratio. In Figs. 5(a) and 5(b) we present the values for P at $E=0$ and $W/V=5$, respectively. We extract them from our simulation data in two separate ways: (a) from the curves $D(E)$ and $D_N(E)$ as plotted in Figs. 2 and 4 (a similar analysis was performed also for $W/V=5$) employing Eq. (12); (b) inserting into (12) $\langle R^2(t_{\max}) \rangle$ and $Z_2(\vec{r}=0, t_{\max})$ for each configuration separately. As seen in Fig. 5(a), both methods yield consistent results for $W/V < 5$. Systematically overestimated values by method (b) in the critical regime could be attributed to the transient time effects and show the necessity for an extrapolation procedure. Note also that for $W=0$, i.e., for a stationary Bloch wave, we are able to evaluate from the definition $P = \frac{2}{3}$. Our results in Fig. 5(a) are consistent with those reported by Weaire and Srivastava⁹ for $W/V < 4$. Their values $P \sim 0.2$ at $W \sim W_c$ could be traced back to the small systems used in their calculations. Our results reveal much lower values $P < 0.1$ in the critical regime and seem to be consistent with the critical ansatz, $P \propto (W_c - W)^\delta$, $\delta \sim 1.4$.

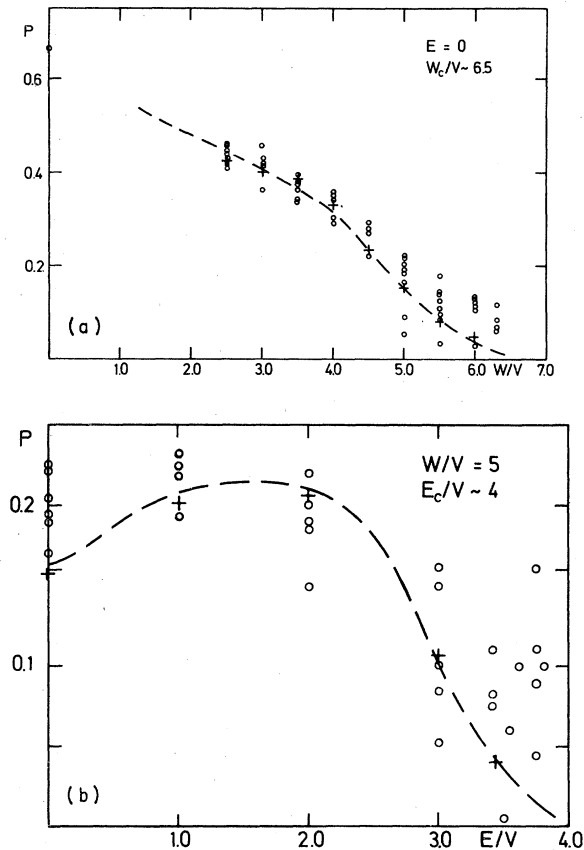


FIG. 5. Participation ratio P at (a) fixed $E=0$ vs W/V and (b) fixed $W/V=5$ vs E/V . Circles represent the results for different configurations as calculated from Eq. (12) and $Z_2(\vec{r}=0, t_{\max})$, $\langle R^2(t_{\max}) \rangle$ without any extrapolations. Crosses denote the values obtained from the average $D_N(E)$ and $D(E)$.

Some results for P in the extended regime have been reported also by Yoshino and Okazaki.⁸ It must be mentioned that they disagree with ours as well as with those of Weaire and Srivastava⁹ already for a weak disorder, e.g., $P \sim 0.25$ at $W/V=2$, which seems to be inconsistent with the exact value at $W=0$. The origin of this discrepancy is not yet clear, therefore we cannot exclude the possibility that the procedure employing the exact eigenstates yields in principle different values for P . Figure 5(b) indicates an analogous critical behavior of P when E is varied, although the results are not so accurate as for the $E=0$ case.

A similar analysis as for P was performed also for higher functions $Z_n(\vec{r}=0, t)$. They confirm the divergence of the eigenfunction amplitude fluctuations at W_c and lend also an additional information about the amplitude distribution. Within our approach it is convenient to study the ratios

$$d_n = F_{n+1}(\vec{r}=0)/[F_n(\vec{r}=0)]^n, \quad (14)$$

$$= \frac{n+1}{2^n} \lim_{t \rightarrow \infty} \frac{Z_{n+1}(\vec{r}=0, t)}{[Z_n(\vec{r}=0, t)]^n},$$

where in the second line Eq. (7) has been used. Note that the d_n , in contrast to $F_n(\vec{r}=0)$, remain finite in the extended as well as in the localized regime. Both limits can be evaluated exactly. Thus, at $W/V \rightarrow \infty$ $d_n \rightarrow 1$, whereas at $W=0$, i.e., for stationary Bloch waves,

$$d_n = 2^{2n+1} \Gamma(n + \frac{3}{2}) / \sqrt{\pi} 3^n \Gamma(n+2), \quad (15)$$

which gives $d_2 = 1.11$, $d_3 = 2.59$, etc. Analysis of our simulation data via (14) yields results which are consistent with both limits and indicate a cusplike behavior in the critical regime. For instance, we obtain at $E=0$ $W/V=6$, $d_2 \sim 3$, and $d_3 \sim 14$, whereas the variation of these quantities with W is approximately linear. Although the scatter of the d_n values at $W \sim W_c$ is not so pronounced as in the case of $D_n(E)$ we are still not in a position to present more quantitative statements about the critical exponents for d_n .

We have also evaluated the ratios $F_n(\vec{r})/F_n(\vec{r}=0)$ in contrast to the d_n do not seem to be affected by the transition and vary smoothly between both limits.

V. CONCLUSIONS

Our main results on the critical behavior in the extended regime can be summarized as follows: (a) The diffusivity $D(E)$ seems to vary continuously in the vicinity of mobility edges. At least our values at fixed E favor the critical ansatz $D(E) \propto (W_c - W)^s$ with $0.7 < s < 1.2$. The data analysis for fixed W/V also indicates a smooth falloff at E_c although the conclusions are less definite. (b) The participation ratio P also exhibits a critical behavior. At $E=0$, e.g., $P \propto (W_c - W)^\delta$ with $\delta \sim 1.4$. Thus, the fluctuations of the eigenfunction amplitudes diverge at W_c which is reaffirmed by the results on $F_n(\vec{r}=0)$ and d_n that reveal a cusplike dependence at $W \sim W_c$.

It has been already recognized⁹ that even conclusion (b) separately would violate the assumption underlying the notion of minimum metallic conductivity. It can be argued that both conclusions are consistent since they essentially confirm the conjecture of Cohen and Jortner¹⁰ that large amplitude fluctuations in the vicinity of mobility edges force the classical percolation behavior of $\sigma(E)$. Similar arguments have been used recently by Mott¹¹ to predict a continuous variation of $\sigma(E)$

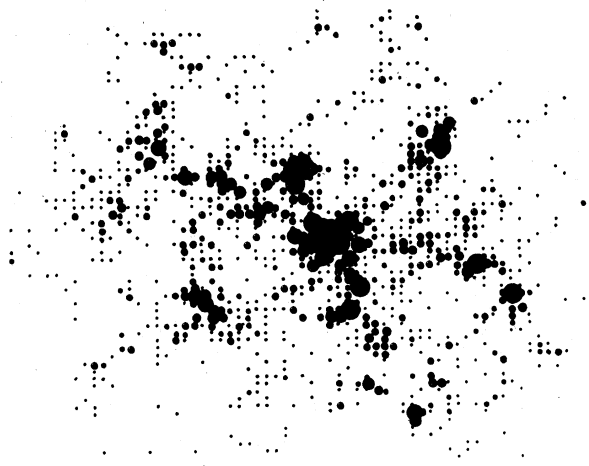


FIG. 6. Snapshot of the particle probability density at $t=180/V > \tau$ for the case $E=0$ and $W/V=6.15$ ($W_c/V \sim 6.5$). The circle areas are proportional to the local values $|\varphi(\vec{r}_i, t)|^2$.

at $W \sim W_c$ although the proposed functional form was not of the ordinary power-law type. To visualize the classical percolation character of the diffusion near the mobility edges we present in Fig. 6 a snapshot of the particle probability density $|\varphi(\vec{r}_i, t)|^2$ at $t \gg \tau$. It can be easily seen that diffusion of the particle has taken place mainly along some rather well pronounced channels. Also, large fluctuations between densities on different sites are recognized. On the other hand, from the minimum-metallic-conductivity concept one would expect a uniform spreading of the wave packet.

The statement on the percolation-type diffusion at W_c does not necessarily lead to the classical percolation value for the exponent s ,²¹ which in two dimensions is $s \sim 1.1$. Our results do not, at least, exclude this possibility. That the quantum-classical analogy is not complete can be concluded also from the participation ratio which represents a quantum counterpart of the site percolation probability.²¹ Here, our value for the critical exponent, $\delta \sim 1.4$, is clearly different from the classical result $\delta < 0.5$.²¹

ACKNOWLEDGMENTS

The research was supported by the Alexander von Humboldt Foundation and in part by the Research Community of Slovenia. The author wishes to thank M. Robnik for his cooperation in the preliminary stages of this work.

- ¹N. F. Mott, *Adv. Phys.* **16**, 49 (1967); N. F. Mott and E. Davis, *Electronic Processes in Noncrystalline Materials* (Clarendon, Oxford, 1971).
- ²D. C. Licciardello and E. N. Economou, *Phys. Rev. B* **11**, 3697 (1975).
- ³F. J. Wegner, *Z. Phys. B* **25**, 327 (1976).
- ⁴A. Aharony and Y. Imry, *J. Phys. C* **10**, L487 (1977).
- ⁵A. Nitzan, K. F. Freed, and M. H. Cohen, *Phys. Rev. B* **15**, 4476 (1977).
- ⁶K. Schönhammer and W. Brenig, *Phys. Lett. A* **42**, 447 (1973).
- ⁷D. C. Licciardello and D. J. Thouless, *Phys. Rev. Lett.* **35**, 1475 (1975); *J. Phys. C* **8**, 4157 (1975).
- ⁸S. Yoshino and M. Okazaki, *J. Phys. Soc. Jpn.* **43**, 415 (1977).
- ⁹D. Weaire and V. Srivastava, *J. Phys. C* **10**, 4309 (1977).
- ¹⁰M. H. Cohen and J. Jortner, *Phys. Rev. Lett.* **30**, 699 (1973); *Phys. Rev. A* **10**, 978 (1974).
- ¹¹N. F. Mott, *Commun. Phys.* **1**, 203 (1976).
- ¹²D. C. Licciardello and D. J. Thouless, *J. Phys. C* **11**, 925 (1978).
- ¹³B. Kramer and D. Weaire, *J. Phys. C* **11**, L5 (1978).
- ¹⁴R. J. Elliott, J. A. Krumhansl, and P. L. Leath, *Rev. Mod. Phys.* **46**, 465 (1974).
- ¹⁵P. Prelovšek, *Phys. Rev. Lett.* **40**, 1596 (1978).
- ¹⁶E. K. Kudinov and Yu. A. Firsov, *Zh. Eksp. Teor. Fiz.* **49**, 867 (1965) [*Sov. Phys. JETP* **22**, 603 (1966)].
- ¹⁷P. N. Butcher, *J. Phys. C* **5**, 3164 (1972).
- ¹⁸N. K. Hindley, *J. Non-Cryst. Solids* **5**, 17 (1970).
- ¹⁹P. Gosar and P. Prelovšek, *Z. Phys.* **266**, 299 (1974).
- ²⁰J. H. Wilkinson and C. Reinsch, *Linear Algebra* (Springer-Verlag, Berlin, 1971).
- ²¹S. Kirkpatrick, *Rev. Mod. Phys.* **45**, 574 (1973).